An Exploration of the Combined Effects of NIR and VIS Spectrally Selective Thermochromic Materials on Building Performance

Runqi Liang[a,b], Yanyi Sun[b], Marina Aburas[b,c], Robin Wilson[b] and Yupeng Wu[b,] *

[a] College of Architecture and Urban Planning, Tongji University, Shanghai, China
[b] Department of Architecture and Built Environment, Faculty of Engineering, The University of Nottingham, University Park, Nottingham, NG7 2RD, UK
[c] School of Architecture and Built Environment, University of Adelaide, Adelaide, South Australia 5005, Australia
*Corresponding author's Email: Yupeng.Wu@nottingham.ac.uk

Abstract

Thermochromic (TC) windows are able to adjust solar radiation transmitted into buildings in response to varying window surface temperature. Vanadium Dioxide (VO_2) is the most common TC material used for TC windows, as it can reduce near infrared (NIR) solar transmittance to block undesirable solar heat gains during hot days when window surface temperature rises above a particular transition temperature. However, few have studied the effect of TC windows on the indoor luminous environment. In order to improve the daylighting control, an innovative Iron-liquid based TC window film which can control the visible (VIS) spectrum was introduced and applied alongside a VO_2 based TC material in this study. The combined performance of these two types of TC materials was discussed under three climatic conditions within China: Beijing, Shanghai and Guangzhou. The results show that enlarging either NIR or visible change, which is the transmittance difference before or after switching, is beneficial for thermochromic performance, the maximum energy saving increased from 11% to 18%, and $UDI_{500\text{-}2000lux}$ is increased by up to 27%. Combined application of NIR and visible spectral selection results in more significant balance between energy and daylighting in demand. While their energy saving potential and daylighting regulating capability affected by the combined implementation is highly dependent on the climate conditions of the TC windows.

Keywords

Thermochromic window; Daylighting; Energy saving; Visible light; NIR light.

1. Introduction

Daylight penetrates through a window system offering illumination as well as heat gain to the indoor environment of a building. The quality and intensity of solar radiation significantly affects the energy consumption of heating, cooling, and lighting, as well as the thermal and visual comfort for occupants in buildings [1-3]. Additionally, daylighting is also beneficial to enhancing mood, increasing productivity, reducing fatigue, and improving human health in general [4, 5]. However, not all of the solar radiation transmitted through windows is desirable; for instance, on hot days, the amount of solar radiation that would need to enter a building to provide sufficient daylighting may simultaneously result in undesirable interior overheating. Nonetheless on cold days, the transmitted solar radiation that is able to heat up the indoor space will reduce heating energy demand, which might result in oversupplied daylighting and an increased risk of visual discomfort (e.g. glare). Therefore, it is essential to have a window system designed in order to attain a balance between thermal and visual comfort when keeping a relative high energy efficiency.

Shading devices and glazing types are the two main components of a window system that can control transmitted solar radiation into the building [6, 7]. By using traditional shading devices, including fixed (passive) [6, 8, 9] and moveable (active) [10-13] shading devices, glare and excessive solar heat gain can be reduced manually or automatically, respectively.

However, the desired daylighting and solar heat gains would be blocked at the same time. It is the full-spectrum solar radiation adjusted by shading devices that restricts the improvement of both thermal and visual comfort.

To improve the window performance in terms of solar heat gain and daylighting control, a variety of glazing technologies have been developed, which are categorised as conventional and smart glazing types. Conventional glazing technologies, such as tinted glazing [14], reflective glazing [15], anti-reflective coated glazing [16], and low-e coated glazing [17], are used to specify the solar transmittance depending on spectrum, reducing over-supply of daylighting (i.e. depending on transmittance within visible spectrum) or solar heat gains (i.e. depending on transmittance within NIR spectrum)[18, 19]. Unlike conventional glazing technologies, innovative smart glazing was explored, which is able to achieve wavelength-dependent adjustment for spectral transmittance depending on specific stimulus. They all have a minimum of two states, which are before and after switching. Once they switch, their visible or NIR transmittance properties can be altered, obtaining a desired daylighting level and thermal comfort inside the building, respectively, the stimulus can be heat (thermochromic), electricity (electrochromic), light (photochromic), or gas (gasochromic) [20]. Gasochromic (GC) glazing switches by filling with diluted hydrogen and reverses by exposure to oxygen, a relatively involved process due to electrolyzer and pipe requirements[21], while thermochromic (TC) and photochromic (PC) glazing systems operate without the requirement for extra power [20, 22]. Currently, the above-mentioned technologies are either at the stage of lab study or small-scale product development (e.g. PC glass for sunglasses), and their potential for regulating daylighting and solar heat gain in buildings continues to be studied [23, 24]. Electrochromic (EC) glazing systems have been widely investigated as well as commercially produced; their reversible switching process is via. a redox reaction powered by DC voltage[25, 26]. Numerical and experimental studies have been conducted to show that EC glazing systems could save lighting energy and reduce discomfort glare by being partially or fully tinted, in place of shading devices [27, 28]. Besides visible transmittance, EC glazing also has the potential to control NIR transmittance (i.e. main part of solar heat gain) simultaneously. Similar to EC glazing, polymer dispersed liquid crystal (PDLC) and suspended particle device (SPD) glazing systems are also electrically actuated. Their state change from coloured/translucent to transparent is caused by variation in particle alignment allowing more light to pass through gaps between particles [29, 30]. PDLC and SPD glazing are both able to control daylight dominantly within the visible spectrum and reduce glare by blocking or diffusing light [30-32]. At this point in time, PDLC device operation cannot be modulated and does not allow vision through its frosted state, whilst VIS and NIR transmittance control range is relatively limited. SPDs, although having a better modulation capacity in comparison to ECs, their notably dark off state leaves them best suited for the windows of vehicles in comparison to those of buildings [21]. Amongst these smart glazing technologies, thermochromic (TC) glazing has the capacity to reversibly transform between two states, named: clear state and tinted state, in response to external and internal environment (mainly thermal environmental), without the need for extra power, according to temperature variations. The most widely studied material is vanadium dioxide (VO_2) [33-35]. The VO_2-based TC glazing switches to a tinted state with a lower NIR transmittance, while keeping its transmittance within the visible spectrum, when it is above transition temperature (T_t). This means that VO_2-based TC glazing is able to block undesired solar heat penetrating into the room, meanwhile providing sufficient daylighting during hot days. Otherwise, TC glazing at clear state admits desired solar heat gains for passive heating during cold days. Many studies have been conducted indicating that VO_2-based TC glazing has the potential to improve buildings' energy efficiency, and thermal comfort, especially under cooling dominated climates [36-40]. However, the daylighting performance affected by

TC windows has rarely been investigated. Meanwhile, the trend of enlarging glazing area in architectural design increases the risk of visual discomfort caused by excessive daylighting (e.g. glare). Therefore, it can be deduced that adjustable visible transmittance is also required for TC windows.

In this study, an innovative iron-liquid based complex film proposed by Wei *et al*. [41] was employed, in order to achieve daylighting adjustment. Unlike other developed thermochromic films, this material features more impressive thermochromic changes within the visible spectrum, as the colour tints from clear to blue with the temperature rising above its transition temperature. Investigation of two types of TC materials: VO_2-based and iron-liquid based TC films were carried out, to explore their effects on indoor luminance and thermal environmental, and building energy consumption, in addition, the requirements for future TC materials development. Under three different climatic conditions (e.g. cold winter and hot summer, mild climate and hot climate), the following scenarios were studied: 1) different TC window transition temperatures; 2) different transmittance; 3) different type of TC windows with various combination between VO_2 based TC and iron liquid based TC.

2. Methodology

A validated building simulation model developed in EnergyPlus has been applied for this study [23, 36]. A typical single office room was used to carry out the prediction of building performance affected by different TCs under three different climates. The energy consumption and useful daylight illuminance (UDI) of the office were analysed to find out the most optimal implement cases for the proposed TC films.

2.1. EnergyPlus model set up

A mid-floor typical single room office of a multi-storeyed building which has the external dimensions of 6m×5m×3m (length × width × height), was modelled in EnergyPlus.

Adjacent offices on the same floor were assumed to be under the same conditions as the studied office. The south-facing wall with a window installed is the surface which is exposed to the outdoor environment. Following the Chinese building regulation, the following setups are used for the building model: The U-value of the south wall is 0.43W/m^{2}K and the U-value of 2.7W/m^{2}K is used for the air filled conventional double-glazed window (dimensions of 4.5m×2m), internal loads include standard equipment and lighting loads that are 13 W/m^2 and 11 W/m^2 respectively. Occupant density is 18.6 m^2/per person. Working hours are taken to be from 9 am to 5 pm on weekdays throughout the year [42]. A constant thermostat temperature of 21ºC is used to controll the HVAC for both winter and summer operating conditions, to minimise the impact of varying indoor temperature when investigating the specific effects of thermochromic windows [43]. The room is divided into two illuminance zones along its depth axis with one close to the window, the other one away from it, to investigate the daylight performance of the proposed thermochromic windows, and explore their impact on artificial lighting energy consumption. One illuminance sensor for each zone is used to achieve automatic dimming control of artificial lighting to meet the target illuminance at work plane of 500lux [44]. These two sensors are placed at 1.5 meters (sensor 1) and 4.5 meters (sensor 2) away from the window, respectively, along with the central axis of the room. Since oversupply of daylighting in area close to the window is the problem that can be relieved by TC window, only the illuminance level at sensor 1 is considered in the following analysis of daylighting performance.

2.2. Material set up

Two type of TC materials were selected for the future building simulation studies: 1) the VO_2 nanoparticle (i.e. VO_2_Nano) film for NIR part of solar raidation control, the spectrum tranmisttance and reflectance of the selected TC materials is shown in Fig 1 (a) [45]. 2) a composite film of Ionic-liquid containing $[bmim]_2\ NiCl_4$ (i.e. TC_IL-Ni^{II}), which has the capability of reducing visible transmittance when its temperature increases from 25 to 75°C [41] as shown in Figure 1 (b).

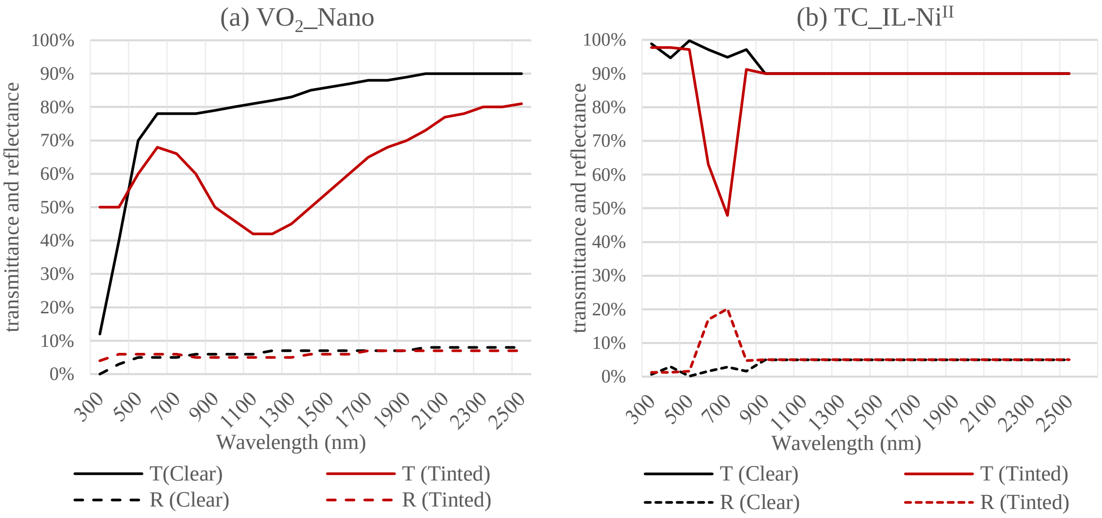

Figure 1: Spectral transmittance and reflectance of VO_2_Nano (a) and TC_IL-Ni^{II}(b).

Each TC film was coated on the inner surface of outside glazing pane within the double-glazing window system in the EnergyPlus model for responding to the outdoor conditions more sensitively [46]. Three scenarios are studied to explore the most appropriate implementation case between the two types of TC films and the material setting in each scenario are outlined as follows:

2.2.1 Scenario I: temperature-dependent

Energy and daylighting performance of buildings with these two TC glazing types installed are studied. Since the thermochromic performance is temperature-dependent, each of VO_2_Nano and TC_IL-Ni^{II} films was numerically analysed in five cases at transition temperatures of 20, 25, 30, 35 and 40 °C, and the corresponding cases labelled as ‘Tt20’, ‘Tt25’, ‘Tt30’, ‘Tt35’and ‘Tt40’, respectively.

2.2.2. Scenario II: spectral transmittance-dependent

According to previous research, restricted transmittance modulation within the NIR or visible spectrum after transition is the key issues that diminishes the thermochromic window performance with respect to energy saving and daylighting adjustment [41, 47]. Therefore, a series of studies improving the modulation degree of NIR or visible transmittance after transition of each TC type were carried out in this scenario. Meanwhile, three different transition temperatures (20, 30 and 40°C) were assigned along with the simulation, in order to investigate the interaction between transition temperature and transmittance modulation. Figure 2 and Table 1 show the settings of the spectral transmittance for all implemented cases.

Table 1: Spectral properties of original and revised VO$_2$_Nano and TC_IL-Ni^{II}

	VO$_2$_Nano					
	Original I		**Case I**		**Case II**	
	Clear	Tinted	Clear	Tinted_M	Clear	Tinted_L
Solar transmittance (τ_{sol})	0.692	0.571	0.692	0.516	0.692	0.385
NIR transmittance (τ_{NIR})	0.819	0.533	0.819	0.394	0.819	0.062
Visible transmittance (τ_{vis})	0.656	0.605	0.656	0.605	0.656	0.605
Absorptance (α)	0.235	0.247	0.235	0.247	0.235	0.247
	TC_IL-Ni ^{II}					
	Original II		**Case III**		**Case IV**	
	Clear	Tinted	Clear	Tinted_M	Clear	Tinted_L
Solar transmittance (τ_{sol})	0.948	0.844	0.948	0.770	0.948	0.631
NIR transmittance (τ_{NIR})	0.914	0.902	0.914	0.890	0.914	0.826
Visible transmittance (τ_{vis})	0.968	0.790	0.968	0.669	0.968	0.471
Absorptance (α)	0.025	0.086	0.025	0.086	0.025	0.086

Figure 2(a) shows the spectral transmittance of two potentially developed VO$_2$_Nano films with different modulation degrees of NIR transmittance after transition. Tinted_M in Case I has moderate reduction of NIR transmittance at tinted state, while Tinted_L in Case II has large reduction of NIR transmittance to 0.062 at tinted state. Both case I and case II have the same optical properties at clear state (i.e. NIR transmittance is 0.819). Accordingly, compared with VO$_2$_Nano film, the change of solar transmittance between clear and tinted state increase by approximately 18% for case I, and 30% for case II. As shown in Table 1, the absorptance at each tinted state of the implemented cases was assumed as constant 0.247, which means that the increase of reflectance that induces the decrease of NIR transmittance.

As shown in Figure 2 (b), two potentially developed TC_IL-Ni^{II} films with different modulation degrees of visible transmittance after transition have been assigned. Tinted_M in Case III shows moderate reduction of visible transmittance to 0.669 at tinted state, and Tinted_L in Case IV has large reduction of visible transmittance to 0.471 at tinted state. Both case III and case IV have the same optical properties at clear state (i.e. visible transmittance is 0.968). Similarly, comparing with the original TC_IL-Ni^{II} film, the change of solar transmittance between clear and tinted state increased by approximately 18% for case III, and 30% for case IV and increases of reflectance results in decrease of visible transmittance.

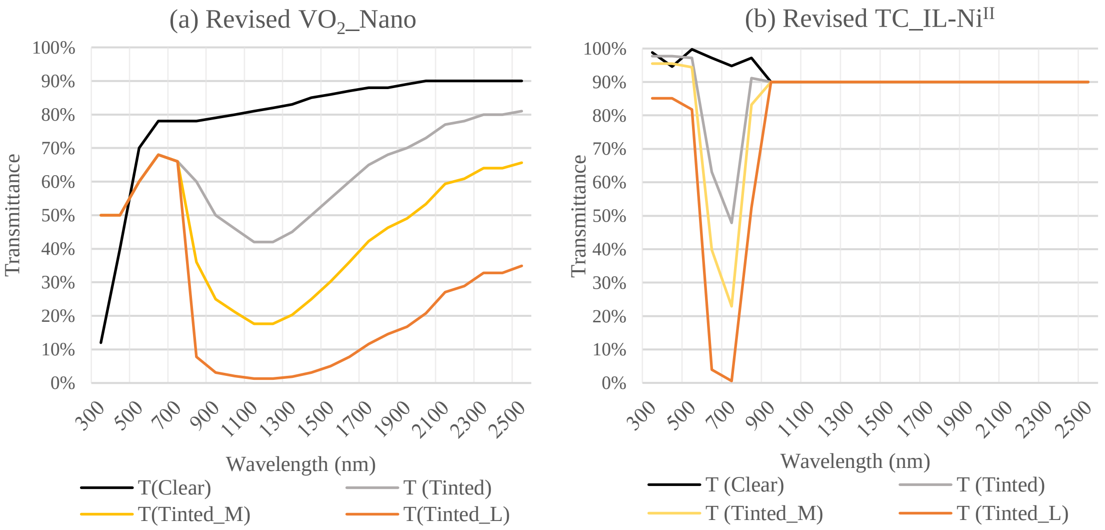

Figure 2: Spectral transmittance of potentially developed VO$_2$_Nano (a) and TC_IL-Ni^{II} (b) with further reduced transmittance.

2.2.3 Scenario III: pairwise combination

Following the studies in scenario II, further exploration was conducted by combining the effects of the VO$_2$_Nano and TC_IL-Ni^{II} films together, in order to find out an appropriate method to control visible and NIR transmittance simultaneously. Within a double-glazing unit, the combination was proposed to be achieved by coating one film on the inner surface of outside glazing pane, and the other on the inner surface of inside glazing pane. The combined implementation cases incorporate the VO_2_Nano film of Case II and the TC_IL-Ni^{II} film of Case IV. Three different transition temperatures for each film, i.e. 20, 30 and 40°C, were considered. According to the transition temperatures for each film, 9 pairwise combined implementation cases of a 3×3 permutation were classified into three groups:

1) VO_2_Nano and TC_IL-Ni^{II} were assumed to have the same transition temperatures of 20°C, 30°C and 40°C, respectively, which were labelled as(Same Tt20) (Same Tt30) (Same Tt40);

2) VO_2_Nano was assumed to have lower transition temperatures than that of TC_IL-Ni^{II}. This means that, during the temperature increase, the transition temperature of VO_2_Nano can be achieved (i.e. decrease of NIR transmittance) first, and then the transition temperature of VO_2_Nano might be achieved (i.e. decrease of visible transmittance). Each implemented case was labelled as 'NIR_20 VIS_30', 'NIR_20 VIS_40' and 'NIR_30 VIS_40', respectively. For instance, 'NIR_20 VIS_30' represents that VO_2_Nano with T_t of 20°C combined with TC_IL-Ni^{II} with Tt of 30°C.

3) TC_IL-Ni^{II} has lower transition temperatures than that of VO_2_Nano. Each implemented case was labelled as 'VIS_20 NIR_30', 'VIS_20 NIR_40', and 'VIS_30 NIR_40', respectively.

2.3. Climates

IWEC (International Weather for Energy Calculation) weather file of Beijing, Shanghai, and Guangzhou (Table 2) respectively was used to conduct this simulation at 15-minute time step intervals for the duration of a year. They are representative climatic conditions of three different zones in China: Beijing represents a cold zone; Shanghai represents a hot summer and cold winter zone; and Guangzhou represents a hot summer and warm winter zone. These three climates all have hot summers with average temperature in the hottest month ranging from 25-30°C. Meanwhile, Beijing has the lowest average temperature, i.e., -2.9°C, in winter. Guangzhou has warm winter with an average temperature of 14°C. Shanghai has a mediate winter with an average temperature of 4.3°C. In addition, these three cities are located at different latitude, resulting in different solar incidence angles. The solar incidence angles from horizontal at 12:00 noon on winter solstice are approximately 27° for Beijing, 35° for Shanghai, and 44° for Guangzhou. A higher solar incident angle means more difficulties for solar radiation approaching the region far away from the vertical window in a building, and less incident solar radiation on the vertical window surface.

Table 2: Climatic properties of three representative cities in difference climate zones of China [48]

Cities	**Location**		**Temperature (Monthly Avg.)**		**Incident Angle at noon (12:00am)**		**Climate Zone**
	Latitude	Longitude	Min.	Max.	Winter solstice	Summer solstice	
Beijing	39.8°N	116.5°E	-2.9°C	26.3°C	27°	73°	Cold
Shanghai	31.2°N	121.4°E	4.3°C	28.2°C	35°	82°	Hot summer and cold winter
Guangzhou	23.1°N	113.3°E	14.0°C	28.9°C	44°	90°	Hot summer and warm winter

3. Results and discussion

Heating, cooling, lighting energy consumption, and daylighting performance that is indicated by useful daylighting illuminance (UDI) of applying different implemented cases of TC windows depicted in these three scenarios were simulated, analysed and discussed in this section. Considering applying them under varying climates, the balance between energy-saving and daylight availability was also investigated.

3.1. Scenario I: Temperature-dependent performance of original TC films

3.1.1. Energy performance

Figure 3 shows the heating, cooling and lighting energy consumption under the implemented cases with original VO_2_Nano and TC_IL-Ni^{II} windows at transition temperatures of 20, 25, 30, 35, 40 and 45°C, respectively. It can be seen that, under all three climates, each case is able to reduce total energy consumption when compared with normal double glazing (DG). And the corresponding energy saving percentages are presented in Table 3.

Various climatic conditions lead to different scales of energy saving potential and different optimum transition temperatures. As shown in Table 3, under the climates of Beijing and Shanghai, 30°C is the optimum transition temperature for original VO_2_Nano window. The maximum energy saving percentages are 10.70% and 11.39%, respectively. While in Guangzhou, the optimum transition temperature is 35°C with 11.49% of energy saving.

As can be seen in Figure 3 (c) and (e), when compared with DG, applying VO_2_Nano window with a low transition temperature of 20 or 25°C increases the lighting energy demand, which diminishes the energy saving caused by reduced cooling energy demand in Shanghai and Guangzhou. Under the climatic conditions of Beijing (Figure 3 (a)), it is the increasing heating demand that converts the tendency of decreasing energy consumption in total, when the VO_2_Nano window has a low transition temperature. This is because that the lower transition temperatures lead to more hours spent on tinted state of VO_2_Nano windows (i.e. relatively lower solar transmittance), which is likely to block the desired solar heat gains and daylighting in heating demand period. However, the VO_2_Nano window with a relatively high transition temperature of 40°C induces more cooling energy consumption than other cases, resulting in restricted total energy saving, as a consequence of fewer hours on tinted state of VO_2_Nano TC film. It means that, during cooling demand period, undesired solar heat gain has not been effectively blocked, which diminishes the capacity of solar spectrum control. Therefore, a moderate transition temperature of 30 or 35°C of VO_2_Nano window enables the balance between hours spent on clear and tinted state, achieving the maximum energy saving, when compared with DG.

In terms of the results affected by TC_IL-Ni^{II} window cases, Figure 3 (b) (d) (f) and Table 3 show that lowering transition temperatures from 40 to 20°C result in a decrease of total energy consumption under all three climates. As can be seen, it is the reduction of cooling energy that results in remarkable total energy saving, and the maximum energy saving compared with DG is 7.47% in Beijing, 6.98% in Shanghai, and 6.20% in Guangzhou. Unlike the VO_2_Nano window cases, heating and lighting energy have not countered the decrease of energy consumption caused by cooling reduction. These results reveal that TC_IL-Ni^{II} window has a relative high solar transmittance (i.e., 0.948 at clear state, 0.844 at tinted state), which restricted the decrease of transmitted solar radiation, thus a further lower solar transmittance is required.

Moreover, data in Table 3 indicates that, at each transition temperature, the VO_2_Nano cases result in more energy saving than TC_IL-Ni^{II} cases, and the difference of their energy saving potential is up to 5.76% in Beijing (Tt35), 6.34% in Shanghai (Tt40), and 7.20% in Guangzhou (Tt40).

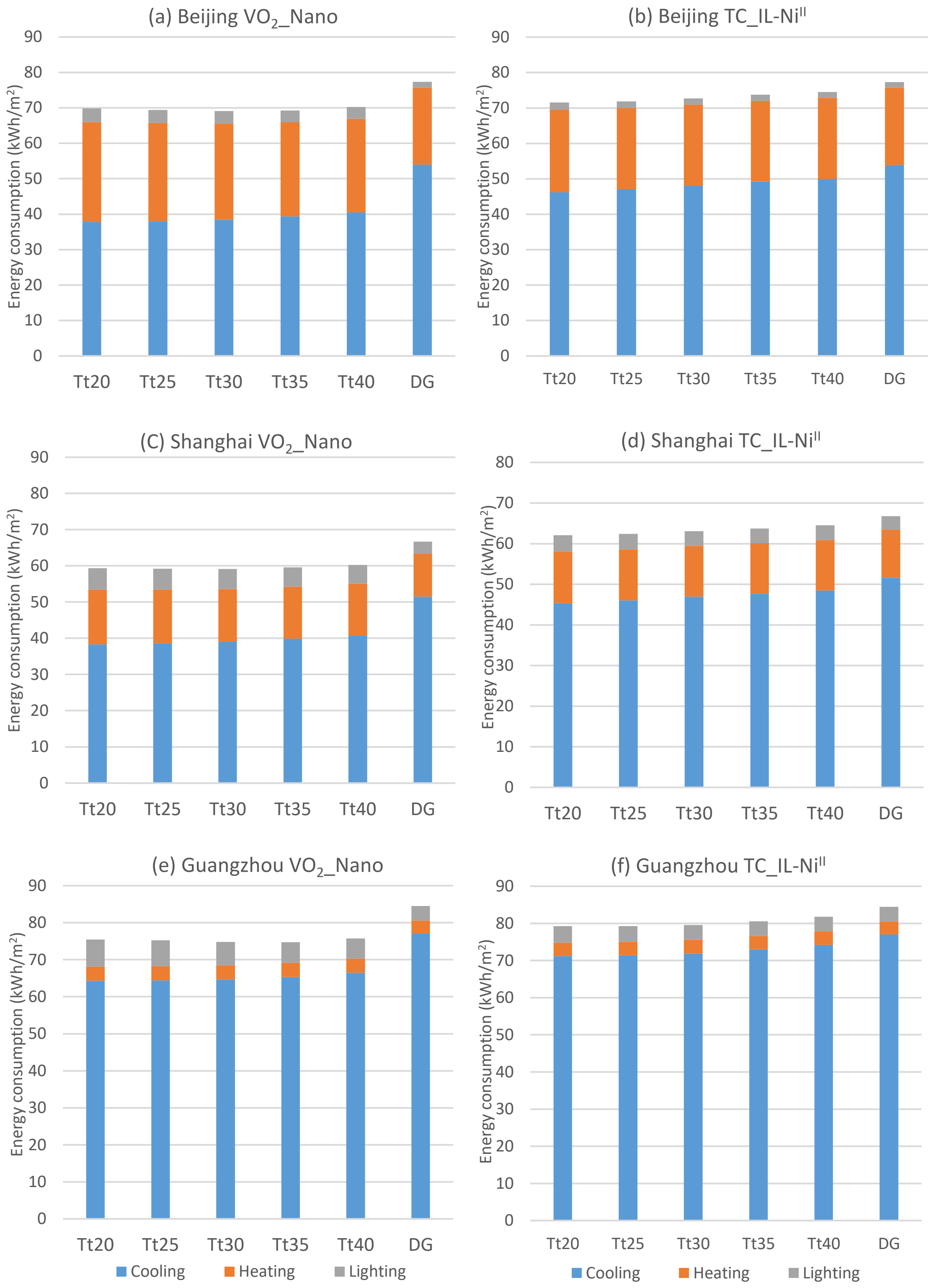

Figure 3. Total energy consumption including heating, cooling, and lighting, classified by windows with different TC materials (i.e. VO_2_Nano and TC_IL-Ni^{II}) and climates (i.e. Beijing, Shanghai and Guangzhou)

Table 3: Summary of energy saving percentage caused by TC windows compared with double glazing

	Energy Saving compared with DG				
	Tt20	**Tt25**	**Tt30**	**Tt35**	**Tt40**

Beijing					
VO_2_Nano	9.68%	10.29%	10.70%*	10.44%	9.22%
TC_IL-Ni^{II}	7.47%*	7.13%	6.03%	4.68%	3.63%
Shanghai					
VO_2_Nano	11.00%	11.31%	11.39%*	10.73%	9.72%
TC_IL-Ni^{II}	6.98%*	6.50%	5.51%	4.54%	3.38%
Guangzhou					
VO_2_Nano	10.67%	10.95%	11.45%	11.49%*	10.36%
TC_IL-Ni^{II}	6.20%*	6.15%	5.80%	4.61%	3.16%

*** The most significant energy saving percentage**

3.1.2. Daylighting performance

Useful daylighting illuminance (UDI) was calculated according to illuminance data output, it represents the percentage of accumulated hours falling in the specific bins of daylighting illuminance levels during the working period. According to occupant preferences and behaviours [49]. Illuminance levels can be classified into three bins: UDI with illuminance lower than 500 lux (UDI$_{<500lux}$); UDI with illuminance between 500 and 2000lux (UDI$_{500\text{-}2000lux}$); UDI with illuminance higher than 2000lux (UDI$_{>2000lux}$) [49]. Among that UDI$_{500\text{-}2000lux}$ was reported as that daylight meets the lighting requirement as the sole source and there's less probability to cause visual and thermal oversupply [49]. Thus, no artificial lighting or shading is required. For an office space, generally, both UDI$_{<500lux}$ and UDI$_{>2000lux}$ are expected to be regulated, since undersupply daylight (UDI$_{<500lux}$) leads to more artificial lighting demand, while oversupply daylight (UDI$_{>2000lux}$) is likely to cause visual or thermal discomfort.

Figure 4 shows the predicted UDI at sensor 1 (i.e. region near the window). It can be seen that oversupplied daylighting, i.e. a high percentage of working hours within UDI$_{>2000lux}$, is the main problem for the region near the window. Both types of TC windows lead to a decrease of UDI$_{>2000lux}$ and increase of UDI$_{500\text{-}2000lux}$ due to their lower visible transmittance than DG. Meanwhile, with the decreasing of transition temperatures, more working hours falling in UDI$_{500\text{-}2000lux}$ bin was detected. It is noted that, a TC_IL-Ni^{II} window results in fewer hours within the $UDI_{500\text{-}2000lux}$ bin than that of a VO_2_Nano window when they have the same transition temperatures. Compared with DG, the VO_2_Nano windows lead to the maximum 15% increase of working hours falling into $UDI_{500\text{-}2000lux}$ bin in Beijing, and that of 27.42% in Shanghai, but only 6.77% in Guangzhou. While under the influence of TC_IL-Ni^{II} window, increase of $UDI_{500\text{-}2000lux}$ compared with DG is restricted, which is up to 3.26%. This is because that the TC_IL-Ni^{II} film has a relatively high visible transmittance (0.968 at clear state, and 0.790 at tinted state). This means that the visible transmittance of TC_IL-Ni^{II} window cases is similar as reference DG. A 17.8% reduction of visible transmittance is not effective to reduce hours falling into the oversupplied $UDI_{>2000lux}$ bin. These results indicated that the lower visible transmittance and transition temperature are both required to improve the daylighting performance.

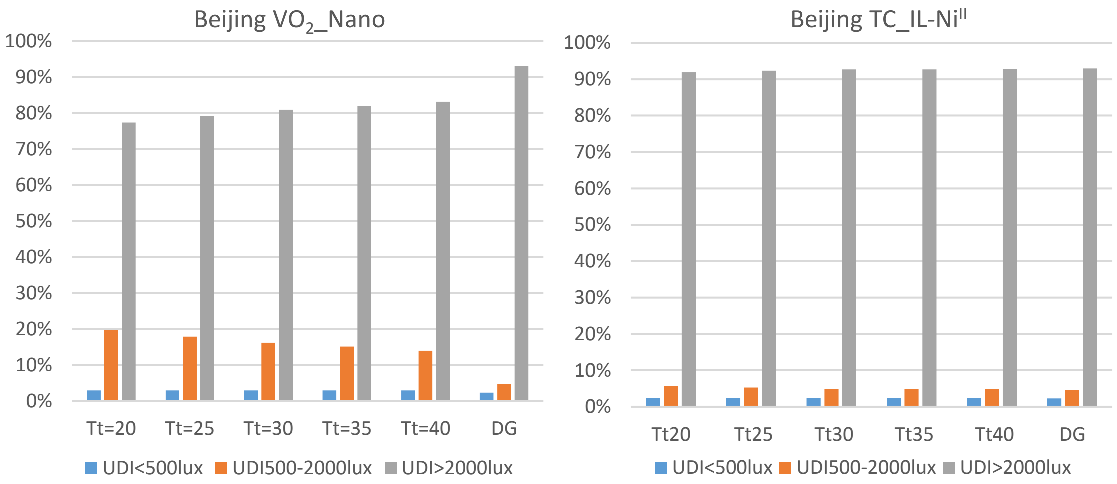

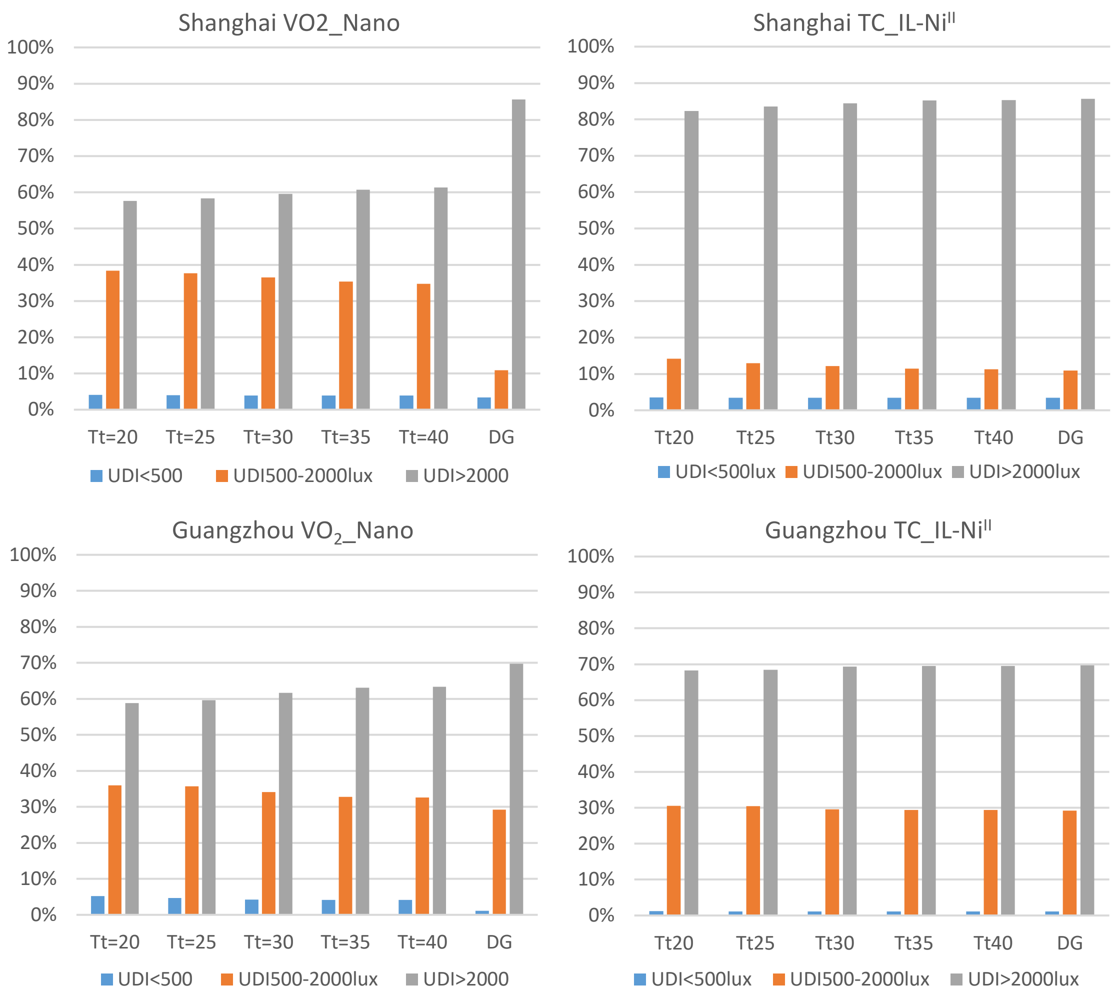

Figure 4: Annual UDI$_{<500lux}$, UDI$_{500-2000lux}$, and UDI$_{>2000lux}$ levels at the sensor 1 affected by VO$_2$_Nano and TC_IL-Ni^{II} TC windows with transition temperatures across 20-40 °C under different climates.

3.2. Scenario II: spectral transmittance-dependent performance of revised TC films

The results of scenario I indicated that the original VO$_2$_Nano and TC_IL-Ni^{II} films have restricted transmittance changes within NIR and visible spectrum respectively, which yield a limited capacity of energy conservation. In this section, the improved VO$_2$_Nano and TC_IL-Ni^{II} windows were investigated, which were assigned with further reduced NIR transmittance and visible transmittance at tinted states, respectively. Moreover, whether the transition temperatures would be affected by the enlarged changes of solar transmittance were explored.

3.2.1. VO_2_Nano cases

Figure 5 presents the predicted energy consumption (see Figure 5(a) (c) (e)) and UDI levels (see Figure 5(b)(d) (f)) affected by improved VO_2_Nano windows. Tint_M cases (i.e. 'Tt20 Tint_M' 'Tt30 Tint_M' and 'Tt40 Tint_M') depicts VO_2_Nano with moderate reduction of NIR transmittance with different transition temperatures. Tint_L cases (i.e. 'Tt20 Tint_L' 'Tt30 Tint_L' and 'Tt40 Tint_L') represents VO_2_Nano with large reduction of NIR transmittance with various transition temperatures.

As can be seen in Figure 5 (a) (c) and (e), Tint_L cases perform more energy efficiently than Tint_M cases at every transition temperature, which is mainly caused by reduced cooling energy consumption. While compared with DG, the Tint_M cases gave rise to a maximum energy conversation at the transition temperature of 30 °C, and the energy saving percentage is 12.6 % in Beijing, 13.0 % in Shanghai, and 13.9% in Guangzhou. In terms of Tint_L cases, the most significant energy saving is achieved when VO_2_Nano window has a transition temperature of 30 °C in Beijing (16.9%) and Shanghai (17.6%), and a transition temperature of 20 °C in Guangzhou (16.0%). These results show that enlarging the change of NIR transmittance between clear and tinted state enables the improvement of energy efficiency. Additionally, the most appropriate transition temperature is 30°C in Beijing and Shanghai, consisting with that of scenario I. However, for the climatic condition of Guangzhou, the most appropriate transition temperature varies a lot according to the variation of optical properties, which is 35°C for original VO_2_Nano window despicted in scenario I , 30°C for Tint_M cases, and 20°C for Tint_L cases. Referring to Figure 5 (e) and 3 (e), it is found that, with the enlarging reduction of NIR transmittance, more energy saving for cooling was achieved in Guangzhou, which counterbalanced the negative effect caused by increasing lighting demand caused by the VO_2_Nano window with a lower transition temperature.

Regarding daylighting performance, Figures 5 (b) (d) and (f) show that the UDI bins distribution of Tint_M cases have no difference with that of Tint_L when they have same transition temperatures. However, the lower transition temperature results in increasing number of working hours falling into the desired illuminance range between 500-2000lux (i.e. $\text{UDI}_{500\text{-}2000\text{lux}}$). Since a lower transition temperature is easily achieved, inducing more hours spent at tinted states with a relative lower visible transmittance, the reduced visible transmittance at tinted state could address the problem caused by oversupplied daylighting, and this trend is consistent with the scenario I as well. Whereas, considering the increasing lighting consumption at the lower transition temperature, a balance between energy and daylighting performance is proposed to be discussed in the following section 3.4.

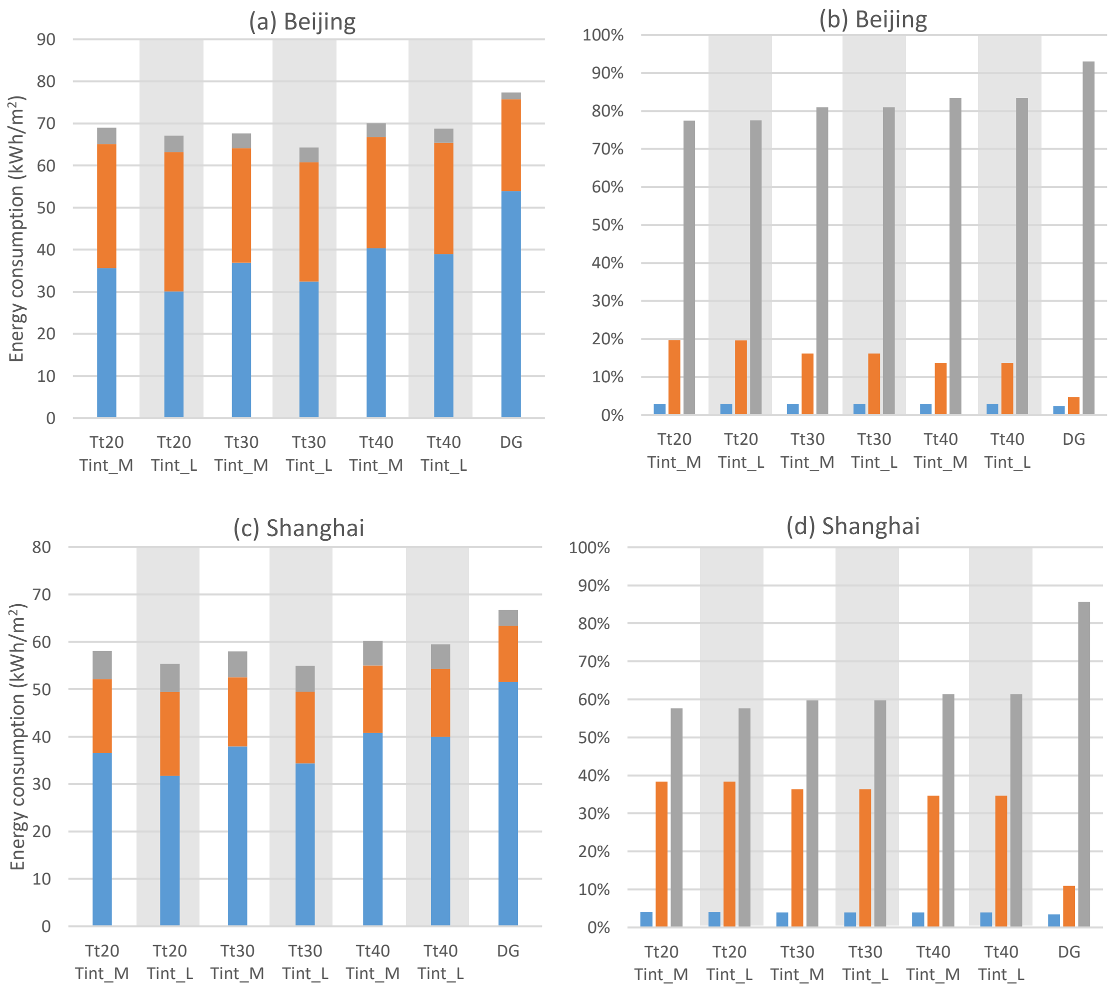

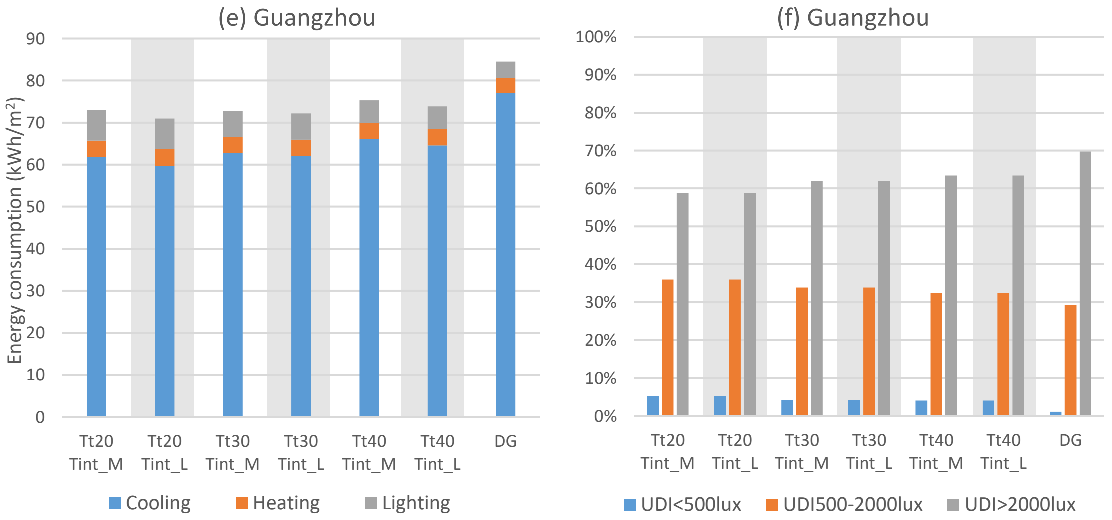

Figure 5. Energy consumption and annual UDI levels at sensor I affected by VO_2_Nano TC windows with different transition temperatures and lower NIR transmittance at tinted state under three climates

3.2.2. TC_IL-Ni^{II} cases

Unlike VO_2_Nano, TC_IL-Ni^{II} has a significant capacity of adjusting the transmittance within the visible spectrum. Figures 6(a), (c) and (e) illustrate the energy performance and Figure 6 (b), (d) and (f) illustrate the daylighting performance affected by improved TC_IL-Ni^{II} under these three climates, respectively. Tint_M cases (i.e. 'Tt20 Tint_M' 'Tt30 Tint_M' and 'Tt40 Tint_M') represnets TC_IL-Ni^{II} with moderate reduction of visible transmittance with various transition temperatures, while Tint_L cases: 'Tt20 Tint_L' 'Tt30 Tint_L' and 'Tt40 Tint_L') depicts TC_IL-Ni^{II} with a large reduction of visible transmittance with various transition temperatures.

Figure 6 (a) (c) and (e) show that, when they have the same transition temperature, Tint_L cases lead to more energy conservation than Tint_M cases. The Tint_M cases with a transition temperature of 20°C lead to the maximum energy saving under each of the three climates, respectively, and the saving accounts for 9.9% in Beijing, 9.4% in Shanghai, and 8.1% in Guangzhou. For the Tint_L cases under the climatic condition of Beijing and Shanghai, it is also the transition temperature of 20°C that induce the most significant energy saving, which is 12.46% in Beijing, and 11.97% in Shanghai. However, in Guangzhou, the Tint_L cases with a transition temperature of 30°C has the maximum energy reduction of 10.6% compared with DG. Unlike Beijing and Shanghai, Tint_L cases in Guangzhou has the more lighting energy consumption at lower transition temperature of 20°C than 30°C, that diminish the energy saving caused by decrease of cooling consumption. It is because that low transition temperature increases the time spent on tinted state with the lower visible transmittance, which reduces the daylight transmitted into the building.

Figure 6 (b) (d) and (f) present that the percentage of working hours falling into the desired $UDI_{500\text{-}2000lux}$ bins increases with the decreasing transition temperature of Tint_M and Tint_L cases, respectively. When the transition temperature is 20 °C, the Tint_L cases have the highest percentage of working hours within 500-2000lux under all three climates. Compared with DG, the increase of $UDI_{500\text{-}2000lux}$ caused by Tint_L cases is up to 14% in Beijing, 22% in Shanghai, and 12% in Guangzhou at the transition temperature of 20°C. Meanwhile, the energy savings of the corresponding cases achieve the peak under the climatic conditions of Beijing and Shanghai. It is means that, Tint_L cases with transition temperature of 20°C are the ideal scenarios giving rise to the most significant daylighting improvement and energy efficiency. Unlike Beijing and Shanghai, under the climates of Guangzhou, the most energy reduction occurs at the transition temperature of 30°C. Therefore, compromises are required to have the ideal scenario: Tint_L with transition temperature of 30°C has the most significant energy saving; Tint_L with transition temperature of 20°C is the most desired daylighting performance.

To sum up, the Tint_L cases for VO_2_Nano and TC_IL-Ni^{II} windows with improved control of NIR and visible transmittance led to more energy conservation. VO_2_Nano windows required a higher transition temperature and induced more energy saving than TC_IL-Ni^{II} windows, but rarely had the capacity of adjusting daylighting. Enlarging the visible transmittance reduction for the TC_IL-Ni^{II} windows could result in an apparent improvement of the desired UDI$_{500\text{-}2000lux}$. However, the high visible transmittance ($\tau_{vis} \approx 97\%$) of the TC_IL-Ni^{II} film at the clear state induced much more oversupply (>2000lux) of daylighting, when compared with VO$_2$_Nano windows.

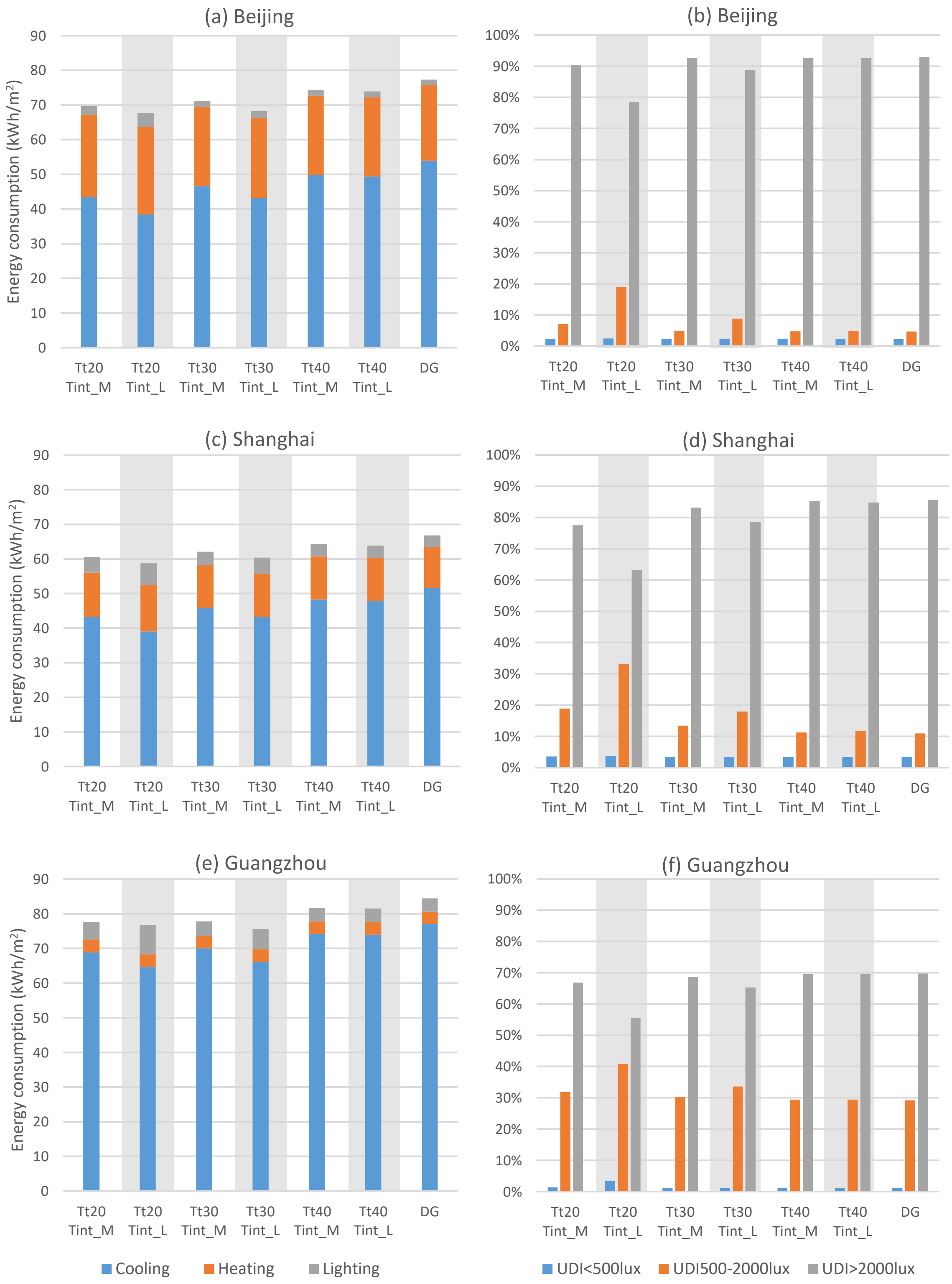

Figure 6: Energy consumption and annual UDI levels at sensor I affected by TC_IL-Ni^{II} TC windows with different transition temperatures and lower visible transmittance at tinted state under three climates

3.3. Scenario III: Performance of pairwise combined application of both TC films

Results in scenario II indicated that the Tint_L cases of VO$_2$_Nano windows are efficient to reduce energy consumption, while the Tint_L cases of TC_IL-Ni^{II} windows are beneficial to adjust daylit conditions. Therefore, a balance between energy and daylighting has the potential to be achieved by combining these two TC materials in the same double-glazing system. In this scenario, energy consumption and UDI distributions affected by nine pairs of combined cases (as depicted in section 2.2.3) of both typical TC materials were predicted through simulation.

Figure 7 shows the results of the combination of TC_IL-Ni^{II} and VO$_2$_Nano with the same transition temperature of 20°C (lablled as 'Same Tt20'), 30°C (lablled as 'Same Tt30') and 40°C (lablled as 'Same Tt40'). Results show that, when transition temperatures of both TC windows are 30°C, the most significant energy saving was achieved in Beijing, which has 14.57% of energy reduction comparing with DG windows. However, the most appropriate combined case is Same Tt40 in Shanghai, reaching maximum energy conservation of 13.50% compared with DG. It can be seen that, under the climatic condition of Beijing and Shanghai, a lower transition temperature could result in more heating demand, which would counter the decreasing trend of total energy consumption caused by cooling decrease with lowering transition temperatures. However, in Guangzhou, heating energy consumption is rarely required. The increase of lighting demand is complementary to the reduction of cooling demand, resulting in similar overall energy consumption for Same_Tt20, Same_Tt30 and Same_Tt40. It reveals that visible and NIR transmittance decreasing simultaneously during TC transition have a positive effect on energy saving. Figure 7 (b) (d) (f) show that, in

Beijing and Shanghai, Same Tt 20 leads to the highest percentage of working hours falling in $UDI_{500\text{-}2000lux}$, which is 48.12% and 63.49%, respectively. While in Guangzhou, the highest $UDI_{500\text{-}2000lux}$ is 64.58% caused by Same Tt30. Unlike Beijing and Shanghai, the case with a transition temperature of 20°C in Guangzhou has a sharp increase of undersupplied $UDI_{<0\text{-}500lux}$, which countered the increase of $UDI_{500\text{-}2000lux}$ with decreasing transition temperature. This is the reason why the Same Tt30 has higher $UDI_{500\text{-}2000lux}$ levels than the Same Tt20 in Guangzhou.

'VIS_20 NIR_30', 'VIS_20 NIR_40', and 'VIS_30 NIR_40' present the cases when the $TC\_IL\text{-}Ni^{II}$ cases have a lower transition temperature than the VO_2_Nano cases. This means that visible transmittance adjusted at a lower temperature than NIR transmittance. Figures 7(a)(c)(e) show that, the cases of 'VIS_30 NIR_40' yields more energy saving, but less improvement of $UDI_{500\text{-}2000lux}$, when compared with DG, than the other two cases in Beijing and Shanghai. However, in Guangzhou, 'VIS_20 NIR_30' leads to the most significant energy saving (13.68% energy reduction compared with DG), and highest value of $UDI_{500\text{-}2000lux}$ among the three cases.

'NIR_20 VIS_30', 'NIR_20 VIS_40', and 'NIR_30 VIS_40' stand for the combined cases with the VO_2_Nano having a lower transition temperature than $TC\_IL\text{-}Ni^{II}$, which means that solar radiation within NIR spectrum transmitted into the room got the adjustment at a lower temperature than that within the visible spectrum. Results in Figure 7(a)(c)(e) present that 'NIR_30 VIS_40' is the most energy efficient case in Beijing and Shanghai, resulting in 17.5% and 15.55% of energy saving compared with DG, respectively. Simultaneously, they are also the cases with the most energy conservation achieved among all cases in this scenario. However, in terms of daylighting performance illustrated in Figure 7 (b) (d) (f), their improvement of $UDI_{500\text{-}2000lux}$ is restricted in Beijing and Shanghai. Under the climatic condition of Guangzhou, 'NIR_20 VIS_30' has the most energy reduction of

17.95%, meanwhile, its percentage of working hours within illuminance 500-2000lux range is approaching 67%, which is higher than any other cases within this scenario.

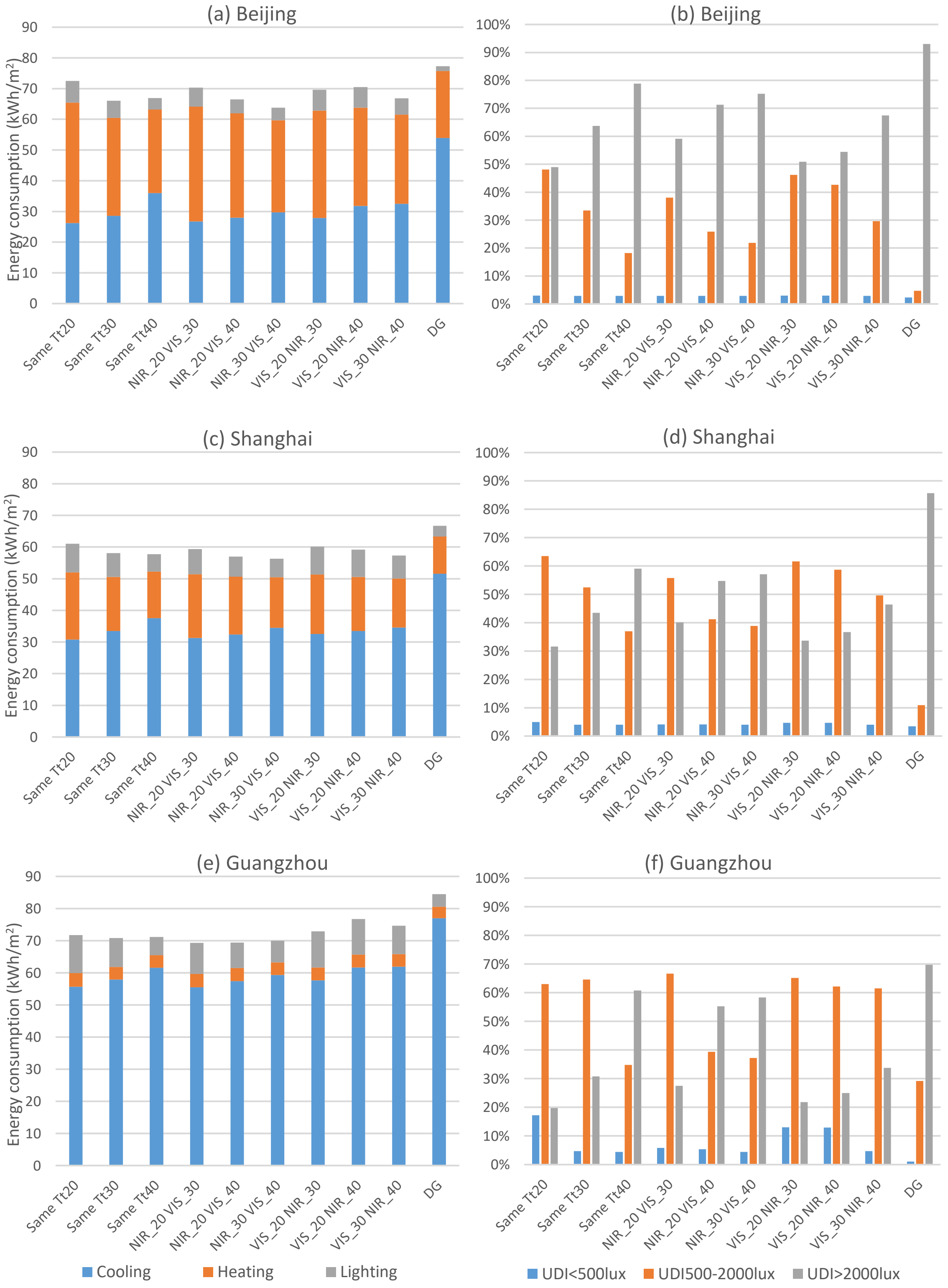

Figure 7. Energy consumption and annual UDI levels at sensor I affected by TC windows of scenario III with different transition temperatures and lower visible transmittance at tinted state under three climates

Under all three climates, the cases of TC_IL-Ni^{II} with a lower transition temperature than VO$_2$_Nano results in more energy consumption than that VO$_2$_Nano has a lower transition temperature. This is because the decrease of visible transmittance has less contribution to reduce the cooling demand inside the building, but resulting in undesired lighting requirement. On the other hand, cooling demand accounts for a larger fraction of the overall energy consumption when compared with lighting demand under each of the three climates. Additionally, reduction of visible lighting transmitted is effective to reduce oversupply illuminance over 2000lux and increase working hours within UDI$_{500\text{-}2000lux}$ bins.

3.4. Discussion about weather conditions and TC performance

Table 4 depicts the energy saving percentages compared with DG affected by the improved VO$_2$_Nano and TC_IL-Ni^{II} windows described in scenario II (Tint_L cases of VO$_2$_Nano or TC_IL-Ni^{II} working on their own) and III (Tint_L cases of VO$_2$_Nano and TC_IL-Ni^{II} working together). It can be seen that some combined cases of both TC materials perform less energy efficiently than using one of them individually. All pairs of the combinations give rise to more working hours falling into the desired illuminance range of 500-2000lux, and the improvement of UDI$_{500\text{-}2000lux}$ compared with DG are rising with the decrease of transition temperatures. Cases with the most significant improvement of daylighting and energy conservation, respectively are highlighted in red within Table 4.

Table 4: Summary of energy saving and improvement of UDI$_{500\text{-}2000lux}$ at sensor I affected by the improved TC windows within scenario II and III

Beijing UDI$_{500\text{-}2000lux}$

TC_IL-Ni^{II} / VO$_2$_Nano		Tt20	Tt30	Tt40
		14.33%	4.15%	0.30%
Tt20	14.87%	**43.43%****	33.30%**	21.15%**
Tt30	11.41%	41.45%**	28.71%**	17.19%**
Tt40	8.99%	37.94%**	24.95%**	13.54%**

Beijing Energy Conservation

TC_IL-Ni^{II} / VO$_2$_Nano		Tt20	Tt30	Tt40
		12.46%	11.81%	4.41%
Tt20	13.31%	6.24%	9.12%	14.06%**
Tt30	16.93%	9.96%	14.57%*	17.50%**
Tt40	11.16%	8.82%	**13.62%****	13.44%**

Shanghai UDI$_{500\text{-}2000lux}$

TC_IL-Ni^{II}	Tt20	Tt30	Tt40

Shanghai Energy Conservation

TC_IL-Ni^{II}	Tt20	Tt30	Tt40

VO$_2$_Nano		22.23%	7.07%	0.89%
Tt20	27.42%	**52.57%****	44.86%**	30.29%**
Tt30	25.40%	50.69%**	41.55%**	27.96%**
Tt40	23.76%	47.78%**	38.69%**	26.04%**

VO$_2$_Nano		11.97%	9.51%	4.39%
Tt20	17.05%	8.48%	11.01%*	14.61%*
Tt30	17.62%	9.96%	12.90%*	15.55%*
Tt40	10.90%	11.27%*	**14.06%****	13.50%**

Guangzhou UDI$_{500\text{-}2000lux}$

TC_IL-Ni^{II} VO$_2$_Nano		Tt20	Tt30	Tt40
		11.71%	4.45%	0.20%
Tt20	6.77%	33.79%**	**37.45%****	10.13%**
Tt30	4.64%	35.97%**	35.38%**	8.05%**
Tt40	3.26%	32.95%**	32.31%**	5.63%**

Guangzhou Energy Conservation

TC_IL-Ni^{II} VO$_2$_Nano		Tt20	Tt30	Tt40
		9.14%	10.59%	3.53%
Tt20	15.98%	15.10%*	**17.95%****	17.80%**
Tt30	14.59%	13.68%*	16.13%**	17.12%**
Tt40	12.63%	9.20%*	11.67%*	15.74%**

* Better performance than VO$_2$_Nano or TC_IL-Ni^{II}, ** Better performance than VO$_2$_Nano and TC_IL-Ni^{II}

Under the climatic conditions of Beijing, the combination between the TC_IL-Ni^{II} case with a transition temperature of 40°C and the VO$_2$_Nano cases with transition temperatures of 20°C, 30°C, and 40°C all have improved performance of energy saving and UDI$_{500\text{-}2000lux}$ increase. Meanwhile, their combination performs better than applying each of them individually. The increase of energy conservation compared with corresponding VO$_2$_Nano windows working on their own is 0.75%, 0.57%, and 2.28%, respectively, while the corresponding increase of UDI$_{500\text{-}2000lux}$ is 6.28%, 5.78%, and 4.55%. Additionally, combining the TC_IL-Ni^{II} cases with a transition temperature of 30°C and the VO$_2$_Nano cases with a transition temperature of 40°C leads to a higher energy conservation of 2.46%, and a higher UDI$_{500\text{-}2000lux}$ of 15.96% than that of VO$_2$_Nano with a transition temperature of 40°C. This means that it is more effective to have the reduction of visible transmittance at a lower temperature instead of NIR transmittance.

The climatic characteristics of Beijing can interpret these results. As Table 5 reports, Beijing has the most hours (866 hrs) falling into the solar incident angle across 20 - 30°, and also has the most accumulated incident solar radiation, where direct daylight accounts for

60%. The most frequent outdoor temperatures are within the range from 0 to 10 °C. This means that even if a large amount of solar radiation is available to enter the building, the outdoor temperature is still low, i.e. early morning or late afternoon in winter days. Therefore, the main issue to address during this period is reducing oversupplied daylighting rather than solar heat gains. That explains why the combination of VO_2_Nano T_t40 and TC_IL-Ni^{II} T_t30 could achieve a balance between energy and daylighting improvement.

Table 4 shows that 2 out of 9 combined cases in Shanghai have better energy and daylighting performance than using the TC_IL-Ni^{II} and VO_2_Nano windows on their own respectively. The paired combination between TC_IL-Ni^{II} Tt40 and VO_2_Nano Tt40 cases results in 13.44% energy conservation, and 26.04% increase of $UDI_{500\text{-}2000lux}$, compared with DG. While the TC_IL-Ni^{II} T_t40 case working with the VO_2_Nano T_t30 case results in energy saving of 14.06%, and a $UDI_{500\text{-}2000lux}$ increase of 38.69%, which are more efficient than the former pair. It means that with the combination of VO_2_Nano T_t40 and TC_IL-Ni^{II} T_t30 there is also the most energy and daylighting efficient case for climate of Shanghai. Moreover, VO_2_Nano with a transition temperature of 20°C or 30°C are more energy efficient (i.e. approx. 17%) than any combination or individually working TC_IL-Ni^{II} cases. Meanwhile, the increase of $UDI_{500\text{-}2000lux}$ is around 27%, which is higher than that in Beijing and Guangzhou. It is indicated that the proposed VO_2_Nano (i.e. Tint_L, Tt of 20°C or 30°C) are suitable for climates in Shanghai.

As described in Table 5, Shanghai has the most hours falling into solar incident angle ranging from 30° to 40°, where direct solar radiation accounts for 50% of the total amount, the outdoor temperature mostly falls within the range of 10-20°C. Compared with Beijing, Shanghai has higher solar incident angles and temperatures, but less solar radiation reaching the window surface. This means that solar radiation within NIR spectrum are more desired to be adjusted than that within visible spectrum. Therefore, VO_2_Nano cases working on their own are able to satisfy the requirements caused by the climatic conditions in Shanghai, which explained the increased energy efficiency induced by VO_2_Nano windows, and their lower transition temperature cases combined with TC_IL-Ni^{II} (VIS_30 NIR_40) having improved the efficiency.

Results in Table 4 show that 5 out of 9 paired combined cases are detected to be significant for both energy conservation and daylighting improvement. The TC_IL-Ni^{II} Tt40 case combining with the VO_2_Nano Tt20, Tt30, and Tt40 cases, respectively, all enable the better energy performance than each of them working on their own. The increase of energy saving compared with the corresponding VO_2_Nano window is 1.82%, 2.53%, and 3.11%, respectively. However, the increase in percentage of working hours within desired $UDI_{500-2000lux}$ is limited, up to 3.41%. The TC_IL-Ni^{II} Tt30 case combined with the VO_2_Nano Tt20 and Tt30 cases, respectively, also results in more energy saving than using each of them individually, and the increase is up to 1.97%. Meanwhile, the working hours within $UDI_{500-2000lux}$ increase significantly by 30%. The results reveal that, in Guangzhou, reducing NIR transmittance at a temperature lower than that of reducing visible transmittance is more effective at achieving both energy saving and desired daylight availability. Additionally, due to the fact that most of the paired combination give rise to increased energy saving, further reduction of NIR transmittance is likely to be required.

Under the climatic conditions of Guangzhou, the most frequent solar incident angle ranges from 40-50°, where the accumulated incident solar radiation is reported to be lower than that of Beijing and Shanghai. Meanwhile, the direct solar radiation occupies 45% of the total. It can be seen that within all solar incident angle ranges, 20-30°C is the outdoor temperature range that the most hours fall within in. This means that Guangzhou dominantly has the high temperatures, but less solar radiation arriving onto the building surface. Therefore, in Guangzhou, reducing solar heat gains by blocking NIR solar radiation is proposed to be the most significant way to reduce dominated cooling energy consumption. This explains the improved energy and daylight performance caused by combining with VO_2_Nano with lower transition temperatures.

Table 5: Climatic conditions of the three cities, including solar incident angles, incident/diffuse solar radiation

Solar Incident Angle (degree)	**0-10**	**10-20**	**20-30**	**30-40**	**40-50**	**50-60**	**60-70**	**70-80**	**80-90**
Beijing									
Frequency (hours)	692	759	886	670	534	433	329	101	0
Accumulated incident solar radiation (W/m^2)	20139	106827	287084	229958	175171	149311	106780	30336	0
Accumulated direct incident solar radiation (W/m^2)	5723	50830	173270	132266	86920	70100	44782	11250	0
Accumulated diffuse incident solar radiation (W/m^2)	12209	46195	89603	72256	62861	54267	41520	12685	0
Temperature (°C) (Hours)	20-30 (198)	0-10 (236)	0-10 (357)	20-30 (218)	20-30 (267)	20-30 (275)	20-30 (244)	20-30 (62)	0
Shanghai									
Frequency (hours)	628	616	671	804	587	481	334	249	30
Accumulated incident solar radiation (W/m^2)	11120	46925	112719	218720	142976	113847	82547	56688	5497
Accumulated direct incident solar radiation (W/m^2)	1931	14556	47310	108594	57120	36896	25437	13799	709
Accumulated diffuse incident solar radiation (W/m^2)	7624	26322	51564	84945	63793	55076	39386	28910	3423
Temperature (°C) (Hours)	20-30 (207)	20-30 (205)	10-20 (218)	10-20 (291)	20-30 (247)	20-30 (251)	20-30 (152)	20-30 (140)	20-30 (27)
Guangzhou									
Frequency (hours)	564	566	558	663	757	466	377	327	108
Accumulated incident solar radiation (W/m^2)	8743	38293	72391	124066	188066	95943	63390	57866	18614
Accumulated direct incident solar radiation (W/m^2)	1559	12843	30089	54093	84716	31427	10042	5385	535
Accumulated diffuse incident solar radiation (W/m^2)	5936	20628	33128	52881	77042	47414	39917	38446	13331
Temperature (°C) (Hours)	20-30 (331)	20-30 (310)	20-30 (306)	20-30 (376)	20-30 (386)	20-30 (289)	20-30 (185)	20-30 (164)	20-30 (58)

4. Conclusions

Based on a typical office room, numerical studies by EnergyPlus simulation were carried out to investigate thermochromic materials working on the windows in a building. Two representative types of TC materials: TC_IL-Ni^{II} (features on visible transmittance change) and VO_2_Nano (features on NIR transmittance change) were selected as porotypes. In order to explore the effects of spectrally selective TC materials within the visible and NIR spectrum on building performance, a series of assumptions were conducted to revise the original TC materials, including varying transition temperatures and enlarging visible or NIR transmittance to reduce oversupplied daylighting and improve energy conservation. These two materials were taken in isolation as well as combination, to explore the ideal pairwise combined applications of both TC materials under the three climates Beijing, Shanghai and Guangzhou. The findings summaried as follow:

1) Both selected TC materials have most suitable transition temperatures depending on the different climates. This is around 30-35°C for VO_2_Nano windows. For TC_IL-Ni^{II} windows, it required a transition temperature of 20°C or less to achieve the most significant energy saving.

2) Both TCs are effective in reducing the oversupplied daylighting in the region near the window. However, because of the original high visible transmittance (i.e. 0.97-0.79) of the TC_IL-Ni^{II} film, it results in the restricted capacity of adjusting visible spectrum.

3) Enlarging the reduction of NIR transmittance for VO_2_Nano, and visible transmittance for TC_IL-Ni^{II} improves the energy efficiency compared with original ones. Meanwhile, the ideal transition temperatures of improved VO_2_Nano and TC_IL-Ni^{II} windows are not affected in Beijing and Shanghai. However, in Guangzhou, the ideal transition temperature of VO_2_Nano decreased with larger NIR spectral reduction, while that of TC_IL-Ni^{II} increased with larger visible spectral reduction.

4) The improved TC_IL-Ni^{II} window has better performance of daylighting adjustment, but is still less efficient than VO_2_Nano, it is because of its high visible transmittance at clear state.

5) Combination of TC_IL-Ni^{II} and VO_2_Nano films led to further improvement of both energy and daylighting performance, and combined methods depend on climatic characteristics:

In Beijing, ‘VIS_30 NIR_40’ is the best case, i.e. reducing the oversupplied daylighting on cold days, and both overlit and overheated conditions on hot days;

In Guangzhou, ‘NIR_40 VIS_30’ is the best case, i.e. reducing the oversupplied daylighting and overheat on hot days, and keeping sufficient daylighting on warm days;

In Shanghai, both improved VO_2_Nano working alone and ‘VIS_30 NIR_40’ have a positive effect, because of its moderatly warm climate.

Acknowledgements

This work was supported by the Faculty of Engineering at the University of Nottingham, UK, through a PhD studentship to Runqi Liang.

References

1. Wong, I.L., *A review of daylighting design and implementation in buildings.* Renewable and Sustainable Energy Reviews, 2017. **74**: p. 959-968.
2. Huang, Y., J.-l. Niu, and T.-m. Chung, *Comprehensive analysis on thermal and daylighting performance of glazing and shading designs on office building envelope in cooling-dominant climates.* Applied Energy, 2014. **134**: p. 215-228.
3. Sun, Y., Y. Wu, and R. Wilson, *Analysis of the daylight performance of a glazing system with Parallel Slat Transparent Insulation Material (PS-TIM).* Energy and Buildings, 2017. **139**: p. 616-633.
4. Edwards，, L. and P. Torcellini, *A Literature Review of the Effects of Natural Light on Building Occupants*. 2002, National Renewable Energy Laboratory: United States.
5. Galatioto, A. and M. Beccali, *Aspects and issues of daylighting assessment: A review study.* Renewable and Sustainable Energy Reviews, 2016. **66**: p. 852-860.
6. Kirimtat, A., et al., *Review of simulation modeling for shading devices in buildings.* Renewable and Sustainable Energy Reviews, 2016. **53**: p. 23-49.
7. Konstantoglou, M. and A. Tsangrassoulis, *Dynamic operation of daylighting and shading systems: A literature review.* Renewable and Sustainable Energy Reviews, 2016. **60**: p. 268-283.
8. Kim, G., et al., *Comparative advantage of an exterior shading device in thermal performance for residential buildings.* Energy and Buildings, 2012. **46**: p. 105-111.
9. Datta, G., *Effect of fixed horizontal louver shading devices on thermal perfomance of building by TRNSYS simulation.* Renewable Energy, 2001. **23**: p. 497-507.

10. Mettanant, V. and P. Chaiwiwatworakul, *Automated Vertical Blinds for Daylighting in Tropical Region.* Energy Procedia, 2014. **52**: p. 278-286.
11. Tzempelikos, A. and H. Shen, *Comparative control strategies for roller shades with respect to daylighting and energy performance.* Building and Environment, 2013. **67**: p. 179-192.
12. Chan, Y.-C. and A. Tzempelikos, *Daylighting and Energy Analysis of Multi-sectional Facades.* Energy Procedia, 2015. **78**: p. 189-194.
13. Tzempelikos, A., *The impact of venetian blind geometry and tilt angle on view, direct light transmission and interior illuminance.* Solar Energy, 2008. **82**(12): p. 1172-1191.
14. Chow, T.-t., C. Li, and Z. Lin, *Innovative solar windows for cooling-demand climate.* Solar Energy Materials and Solar Cells, 2010. **94**(2): p. 212-220.
15. Cuce, E. and S.B. Riffat, *A state-of-the-art review on innovative glazing technologies.* Renewable and Sustainable Energy Reviews, 2015. **41**: p. 695-714.
16. Rosencrantz, T., et al., *Increased solar energy and daylight utilisation using anti-reflective coatings in energy-efficient windows.* Solar Energy Materials and Solar Cells, 2005. **89**(2-3): p. 249-260.
17. Leftheriotis, G. and P. Yianoulis, *Glazings and Coatings.* Comprehensive Renewable Energy, 2012. **3**: p. 313-355.
18. Sun, Y., et al., *Glazing systems with Parallel Slats Transparent Insulation Material (PS-TIM): Evaluation of building energy and daylight performance.* Energy and Buildings, 2018. **159**: p. 213-227.
19. Sun, Y., et al., *Development of a comprehensive method to analyse glazing systems with Parallel Slat Transparent Insulation material (PS-TIM).* Applied Energy, 2017. **205**: p. 951-963.
20. Granqvist, C.G., et al., *Advances in chromogenic materials and devices.* Thin Solid Films, 2010. **518**(11): p. 3046-3053.
21. Casini, M., *Active dynamic windows for buildings: A review.* Renewable Energy, 2018. **119**: p. 923-934.
22. Feng, W., et al., *Gasochromic smart window: optical and thermal properties, energy simulation and feasibility analysis.* Solar Energy Materials and Solar Cells, 2016. **144**: p. 316-323.
23. Liang, R., et al., *Evaluation of the thermal and optical performance of thermochromic windows for office buildings in China.* Energy and Buildings, 2018. **176**: p. 216-231.
24. Liang, R., et al., *Investigation of Mg-Y coated gasochromic smart windows for building applications.* Building Simulation, 2018. **12**(1): p. 99-112.
25. Granqvist, C.G., et al., *Progress in chromogenics: New results for electrochromic and thermochromic materials and devices.* Solar Energy Materials and Solar Cells, 2009. **93**(12): p. 2032-2039.
26. Ghosh, A. and B. Norton, *Advances in switchable and highly insulating autonomous (self-powered) glazing systems for adaptive low energy buildings.* Renewable Energy, 2018. **126**: p. 1003-1031.
27. Fernandes, L.L., E.S. Lee, and G. Ward, *Lighting energy savings potential of split-pane electrochromic windows controlled for daylighting with visual comfort.* Energy and Buildings, 2013. **61**: p. 8-20.
28. Piccolo, A., *Thermal performance of an electrochromic smart window tested in an environmental test cell.* Energy and Buildings, 2010. **42**(9): p. 1409-1417.
29. Ghosh, A., B. Norton, and T.K. Mallick, *Influence of atmospheric clearness on PDLC switchable glazing transmission.* Energy and Buildings, 2018. **172**: p. 257-264.

30. Ghosh, A. and B. Norton, *Optimization of PV powered SPD switchable glazing to minimise probability of loss of power supply.* Renewable Energy, 2019. **131**: p. 993-1001.
31. Ghosh, A. and T.K. Mallick, *Evaluation of colour properties due to switching behaviour of a PDLC glazing for adaptive building integration.* Renewable Energy, 2018. **120**: p. 126-133.
32. Ghosh, A., B. Norton, and T.K. Mallick, *Daylight characteristics of a polymer dispersed liquid crystal switchable glazing.* Solar Energy Materials and Solar Cells, 2018. **174**: p. 572-576.
33. Zhou, S., et al., *Microstructures and thermochromic characteristics of low-cost vanadium–tungsten co-sputtered thin films.* Surface and Coatings Technology, 2012. **206**(11-12): p. 2922-2926.
34. Li, S.-Y., G.A. Niklasson, and C.G. Granqvist, *Thermochromic undoped and Mg-doped VO2 thin films and nanoparticles: Optical properties and performance limits for energy efficient windows.* Journal of Applied Physics, 2014. **115**(5): p. 053513.
35. Huang, Z., et al., *Tungsten-doped vanadium dioxide thin films on borosilicate glass for smart window application.* Journal of Alloys and Compounds, 2013. **564**: p. 158-161.
36. Ye, H., et al., *The demonstration and simulation of the application performance of the vanadium dioxide single glazing.* Solar Energy Materials and Solar Cells, 2013. **117**: p. 168-173.
37. Long, L. and H. Ye, *Discussion of the performance improvement of thermochromic smart glazing applied in passive buildings.* Solar Energy, 2014. **107**: p. 236-244.
38. Saeli, M., et al., *Energy modelling studies of thermochromic glazing.* Energy and Buildings, 2010. **42**(10): p. 1666-1673.
39. Hoffmann, S., E.S. Lee, and C. Clavero, *Examination of the technical potential of near-infrared switching thermochromic windows for commercial building applications.* Solar Energy Materials and Solar Cells, 2014. **123**: p. 65-80.
40. Ye, H. and L. Long, *Smart or not? A theoretical discussion on the smart regulation capacity of vanadium dioxide glazing.* Solar Energy Materials and Solar Cells, 2014. **120**: p. 669-674.
41. Wei, X., et al., *Solar-thermochromism of Pseudocrystalline Nanodroplets of Ionic Liquid-Ni Complexes immobilized inside translucent Microporous PVDF Films.* Advanced Materials, 2009. **21**: p. 776-780.
42. Construction, M.o. and I.a.Q. General Administration of Quality Supervision, *GB50189-2005 Design Standard for Energy Efficiency of Public Buildings*. 2005, Ministry of Construction.
43. CIBSE, *GuideA: Environmental design*. 1999, The Chartered Institution of Building: Services Engineers London.
44. BSI, *BS EN 12464-1:2011 Light and lighting - Lighting of work places. Indoor work places*. 2011, BSI Stardard.
45. Li, S., *VO2-based Thermochromic and Nanothermochromic Materials for Energy-Efficient Windows,* in *Science and technology, Uppsala University*. 2013. p. 142.
46. Chen, X., Q. Lv, and X. Yi, *Smart window coating based on nanostructured VO2 thin film.* Optik - International Journal for Light and Electron Optics, 2012. **123**(13): p. 1187-1189.
47. Gao, Y., et al., *Enhanced chemical stability of VO2 nanoparticles by the formation of SiO2/VO2 core/shell structures and the application to transparent and flexible VO2-based composite foils with excellent thermochromic properties for solar heat control.* Energy & Environmental Science, 2012. **5**(3): p. 6104.

48. ASHRAE, *International Weather for Energy Calculations (IWEC Weather Files) Users Manual and CD-ROM* 2001: ASHRAE, Atlanta.

49. Nabil, A. and J. Mardaljevic, *Useful daylight illuminances: A replacement for daylight factors.* Energy and Buildings, 2006. **38**(7): p. 905-913.